Cytotherapy 26 (2024) 1320–1330

Contents lists available at ScienceDirect

CYTOTHERAPY

journal homepage: www.isct-cytotherapy.org

FULL-LENGTH ARTICLE
Immunotherapy

IL-27-engineered CAR.19-NK-92 cells exhibit enhanced therapeutic efficacy

Alison Felipe Bordini Biggi[1,#], Renata Nacasaki Silvestre[1,#], Mariane Cariati Tirapelle[1], Julia Teixeira Cottas de Azevedo[1,2], Henry David Mogollón García[3], Matheus Henrique dos Santos[1], Sarah Caroline Gomes de Lima[1], Lucas Eduardo Botelho de Souza[1], Dimas Tadeu Covas[1], Kelen Cristina Ribeiro Malmegrim[1,4], Marxa L. Figueiredo[5], Virginia Picanço-Castro[1,*]

[1] *Center for Cell-based Therapy CTC, Regional Blood Center of Ribeirão Preto, University of São Paulo, São Paulo, Brazil*
[2] *Department of Hemotherapy and Cellular Therapy, Hospital Israelita Albert Einstein, São Paulo, Brazil*
[3] *Universidade Estadual de Campinas, Instituto de Biologia, São Paulo, Brazil*
[4] *Department of Clinical Analyses, Toxicology and Food Science, School of Pharmaceutical Sciences of Ribeirão Preto, University of São Paulo, Ribeirão Preto, Brazil*
[5] *Department of Basic Medical Sciences, Purdue University, West Lafayette, Indiana, USA*

ARTICLE INFO

Article History:
Received 11 December 2023
Accepted 1 June 2024

Key Words:
blood cancer
CAR-NK
IL-27
immunotherapy
NK-92

ABSTRACT

Chimeric antigen receptor (CAR) engineering of natural killer (NK) cells has shown promising results in early-phase clinical studies. However, advancing CAR-NK cell therapeutic efficacy is imperative. In this study, we investigated the impact of a fourth-generation CD19-targeted CAR (CAR.19) coexpressing IL-27 on NK-92 cells. We observed a significant improvement in NK-92 cell proliferation and cytotoxicity activity against B-cell cancer cell lines, both *in vitro* and in a xenograft mouse B-cell lymphoma model. Our systematic transcriptome analysis of the activated NK-92 CAR variants further supports the potential of IL-27 in fourth-generation CARs to overcome limitations of NK cell-based targeted tumor therapies by providing essential growth and activation signals. Integrating IL-27 into CAR-NK cells emerges as a promising strategy to enhance their therapeutic potential and elicit robust responses against cancer cells. These findings contribute substantially to the mounting evidence supporting the potential of fourth-generation CAR engineering in advancing NK cell-based immunotherapies.

Introduction

Chimeric antigen receptor-natural killer (CAR-NK) cells have been emerging as a promising cell therapy. CAR-NK cells retain an intrinsic ability to recognize and direct their cytotoxicity to tumor cells through their native receptors, making tumor cell evasion less likely through down-regulation of the target antigen of CAR [1]. Due to its repertoire of cytokines (e.g., IFN-γ and GM-CSF [2]), cytokine release syndrome is less frequent in CAR-NK-based therapy [3], unlike T-cells, which produce large amounts of inflammatory cytokines (e.g., TNFα, IL-6 and IL-1) [4]. In addition to their CAR-dependent antitumor response, NK cells maintain their CAR-independent antitumor capacity, for example, by the balance between the expression of costimulatory (e.g., DNAM-1) and inhibitory (e.g., NKG2A) checkpoints [5]. Also, by not expressing the T-cell receptor, NK cells generally do not cause graft-versus-host disease, which renders CAR-NK cells excellent candidates for allogeneic (off-the-shelf) therapeutic use [6].

However, despite the promising therapeutic potential of NK cells, their translation into clinical applications faces significant challenges. These obstacles encompass their restricted capacity for expansion, both in laboratory settings and within the body, along with the need to sustain their cytotoxic capabilities [7]. Consequently, to broaden the antitumor applications of CAR-NK cells, a novel strategy that empowers these cells to surmount the hostile tumor microenvironment and persist *in vivo* would be beneficial.

IL-27 is a heterodimeric cytokine that belongs to the IL-12 family and is composed by a heterodimer of IL27A (p28) and IL27B (Epstein-Barr virus-induced gene 3 or EBI3), with IL-27Rα (WSX1) and gp130 (IL6ST) as a heterodimeric receptor [8]. When combined with other

* Correspondence: Virginia Picanço-Castro, PhD, Center for Cell-based Therapy CTC, Regional Blood Center of Ribeirão Preto, University of São Paulo, Ribeirão Preto, São Paulo, 14051-140, Brazil.
E-mail address: virginia.picanco@hemocentro.fmrp.usp.br (V. Picanço-Castro).
# These authors contributed equally to this work.

https://doi.org/10.1016/j.jcyt.2024.06.001

cytokines (e.g., IL-15, IL-18), IL-27 modulates the antitumor cytotoxic response of NK cells by inducing the expression of activating receptors on NK cells, including NKp46, NKG2D, NKp44, NKp30 and CD69. In addition, IL-27 stimulates IFN-γ production, thereby enhancing the cytotoxicity of NK cells [9,10].

IL-27 has an essential role in promoting the interaction of the innate and adaptive immunity responses in its antitumor effects. IL-27 can both enhance the cytotoxic activity of NK cells and increase the susceptibility of tumor cells to NK cell-mediated cytotoxicity. IL-27 also cooperates with antibody-dependent cell-mediated cytotoxicity (ADCC) activity and increases the expansion of cytotoxic T-cells by inducing the expression of transcription factors T-bet and eomesodermin [11]. In several tumor studies, it has been demonstrated that IL-27 increases the cytotoxic response of NK cells against different tumor lineages, by a variety of mechanisms, including those dependent on perforin, granzymes, TRAIL and Fc-γR-III, for example [9,10]. In human follicular lymphoma, and diffuse large B-cell lymphoma models, it has been demonstrated that neoplasic B-cells have functional IL-27 receptors and that IL-27 can potentiate antitumor toxicity *in vitro* and *in vivo* [12]. In T cells, mechanisms related to IL-27 function are better detailed, being related to the activation of STAT1 and STAT3 pathways [13,14]. In a colon carcinoma model, transduction of the C26 cell line with IL-27 prior to implantation enabled induction of strong IFN-γ production and cytotoxic T-cell antitumor responses [15]. In a nanoparticle intratumoral delivery system, IL-27 induced robust infiltration of immune effector cells when combined with IL-12 and was able to effectively inhibit tumor growth [16].

Although many studies point to IL-27 activity within tumors, we sought to better understand the molecular mechanisms associated with IL-27 expression in NK cells and their role in promoting cytotoxicity. Therefore, we postulated that CAR-NK cells, with a constitutive expression and secretion of IL-27, could significantly improve the survival and anti-tumor activity of CAR.19 NK-92 cells, both *in vitro* and *in vivo*. Our results underscore the potential of IL-27 engineering in CAR.19 NK-92 cells, marking a substantial advance for CAR-NK cell-based immunotherapies.

Material and Methods

Cell lines

NK-92 cells (ATCC CRL-2407, Manassas, Virginia) were cultured in X-VIVO 10 media (Lonza - Basel, Switzerland) supplemented with 5% human AB plasma and 500 IU/mL of IL-2 (Proleukin - Clinigen, Yardley, Pennsylvania) at a concentration of 1×10^5 cells/mL, 37°C and 5% CO_2. Raji, NALM-6 and K562 cell lines were cultured in RPMI 1640 media (ThermoFisher - Waltham, Massachusetts) supplemented with 10% fetal bovine serum (ThermoFisher) at a concentration of 2.5×10^5 cells/mL, 37°C and 5% CO_2.

Short tandem repeat (STR) profiling

All cell lines underwent authentication through STR analysis of eight major STR loci targeted for identification, namely D5S818, D7S820, CSF1PO, vWA, D16S539, TPOX, THO and D13S317. Specific primers for each locus were used in conjunction with a PCR amplification kit (Sigma-Aldrich - San Luis, Missouri). Subsequently, electrophoretic analysis with polyacrylamide gel was conducted, and the resulting bands were stained with silver nitrate. The obtained STR profiles were then analyzed to ensure cell line integrity and validity.

CAR constructs

The second-generation anti-CD19 CAR consisted of CD8 hinge/-transmembrane, and 4-1BB-CD3ζ intracellular signaling domains (henceforth CAR.19), while the fourth-generation anti-CD19 CAR included the same components along with the IL-27 (human hyper-IL-27 cDNA from pORF9-mEBI3/p28—Invivogen - San Diego, California) gene sequence (henceforth CAR.19-IL-27). Both CAR constructs were under the control of the SFFV promoter and were cloned into the lentiviral vector. To generate lentiviral vectors, 293T cells (ATCC CRL-3216) were cotransfected with the lentiviral vector (CAR.19 or CAR.19-IL-27), along with auxiliary packaging plasmids, psPAX2 and pMD.2G, using PEI reagent. Supernatant was collected after 48 and 72 h, centrifuged at $450 \times g$ for 5 min at 4°C, and concentrated with Lenti-X (Takara - San Jose, California). Lentivirus functional titer was assessed by transducing K562 cells and analyzed by flow cytometry. Two CAR-NK cell variants were generated from the NK-92 cells (control): CAR.19 (NK-92 cells expressing CAR.19) and CAR.19-IL-27 (NK-92 cells expressing CAR.19 and IL-27).

Transduction and selection of CAR-NK-92 cells

NK-92 cell transduction used polybrene (8 μg/mL) and BX795 (16μM). Spinoculation followed at $1000 \times g$ for 60 min, with medium replenished after 6 h. Transduction efficiency assessed via flow cytometry after 48 h using specific and isotype control antibodies. CAR-positive cells isolated using Biotin-SP-conjugated anti-CAR-CD19 antibody and antibiotin Microbeads. Magnetic column separation retained CAR-positive cells from the culture.

NK-92 cells immunophenotyping

To analyze the immunophenotypic profile of NK-92, CAR.19 and CAR.19-IL-27 cells, the following BD Biosciences (Franklin Lakes, NJ, USA) monoclonal antibodies were used for staining: CD56, CD3, CD45, CD28, CD16, CD11a, CD2, NKG2D, NKp30, NKp46, DNAM-1, CD95 and 7-AAD viability dye. CAR-positive cells were further stained with Alexa Fluor 647 AffiniPure $F(ab')_2$ Fragment Goat Anti-Mouse IgG, $F(ab')_2$ fragment specific (Jackson Immunoresearch - West Grove, Pennsylvania), and Alexa Fluor 647 ChromPure Goat IgG, $F(ab')_2$ fragment (Jackson Immunoresearch) as isotype control. Subsequently, samples were analyzed using the BD LSR Fortessa Cell Analyzer cytometer (BD Biosciences - Franklin Lakes, New Jersey).

In vitro *cytotoxicity and cytokine release assay*

Raji (CD19+), NALM-6 (CD19+) and K562 (CD19−) cells were labeled with PKH67 (Merck - Rahway, New Jersey). Effector and target cells were co-cultured in 96-well plates at 2:1 effector:target (E:T) ratio. Cytotoxicity was measured by assessing the difference in viable PKH67-positive cells at time 0 and after 5 h.

IL-27, granzyme A and B, perforin and IL-8, 10 and 18 were analyzed through a multiplex assay using the MILLIPLEX Human Cytokine/Chemokine/Growth factor Panel A kits (Merck—HCYTA-60K) and the MILLIPLEX MAP Human CD8+ T-Cell Magnetic Bead Panel (Merck—HCD8MAG-15K). The assay plate was then analyzed using the MAGPIX system (Luminex - Austin, Texas). IFN-γ and TNFα levels were analyzed by ELISA following the manufacturer's protocol (BD Biosciences).

CD107 degranulation assay

NK cell degranulation was assessed by staining for CD107a (LAMP-1) during NK cell stimulation. NK-92 cells (3×10^5 cells/well) were incubated in 96-well plates for 5 h as control, and for targeted stimulation, they were co-cultured with Raji, Nalm-6 and K562 cells at a concentration of 1.5×10^5 (2:1 E:T ratio). To evaluate degranulation, the anti-CD107a-PE antibody (BD Biosciences) or isotype control was added to the NK-92 cells, allowing binding to the degranulation marker as granules were exocytosed. After the first hour of culture, 2 μM of monensin (Sigma-Aldrich) was added to each well. CD56

and 7-AAD staining was performed before flow cytometry analysis, focusing on the live CD56+ gated population to assess NK-92 cell degranulation by expression of CD107a.

ERK1/2 phosphorylation and apoptosis assay

To detect phosphorylated ERK1/2, effector cells were cultured alone or at a 1:1 (E:T) cell ratio with target cell line Raji for activation of effector cells (5×10^5 each/well), without IL-2. Cells were incubated at 37°C for 25 min, stained with Fixable Viability Stain (FVS) 575V (BD) for 5 min at 37°C, and then fixed with Phosflow Fix Buffer I (BD) (30 min after co-culture). Cells were washed twice with Phosflow Perm/Wash Buffer I (BD), resuspended in 300 μL of Phosflow Perm Buffer III (BD), and incubated on ice for 30 min. Washed twice, and stained with CD56 (PE-CF594/BD), and antiphospho-ERK1/2 (Thr202, Tyr204) antibody (Alexa 488/BioLegend), for 30 min at 4°C, in Perm/Wash Buffer I. Cells were washed and analyzed by FACS, focusing on the FVS-CD56+ gated population. For apoptosis assay, cells were cultured in the same conditions as the RNAseq, 10:1 (E:T) ratio for 24 h, washed and stained with anti-Annexin-V (FITC) and 7-AAD and incubated for 15 min at RT in the dark. Then, cells were resuspended in 300 μL of 1X Binding Buffer (BD) and analyzed by FACS.

RNAseq

RNA from CAR.19 and CAR.19-IL-27 cells were extracted using the RNeasy Plus Micro kit (Qiagen—Hilden, Germany) and measured on a Nanovue (GE Healthcare - Chicago, Illinois) spectrophotometer. For each sample, RNA was extracted before and after the cytotoxicity assay, in which cells were cultured at a 10:1 (E:T) ratio for 24 h, to ensure complete lysis of target cells (Figure S1). Poly(A) RNA sequencing library was prepared following Illumina's TruSeq-stranded-mRNA protocol and conducted by LC Sciences (Houston, TX, USA). Poly(A) tail-containing mRNAs were purified using oligo-dT. Briefly, mRNA was extracted using magnetic beads with two rounds of purification and then fragmented using a divalent cation buffer at an elevated temperature. Quality control analysis and quantification of the sequencing library were performed using an Agilent Technologies 2100 Bioanalyzer High Sensitivity DNA Chip. Paired-end sequencing was performed on Illumina's NovaSeq 6000. For transcript assembly and estimating transcript expression levels, the software is described by Figueiredo et al. [17]. For differential expression analysis of mRNAs, StringTie was used by calculating fragments per kilobase million (FPKM). The differentially expressed mRNAs in CAR.19-IL-27 and CAR.19 were selected with log2 (fold change) > 1.5 or log2 (fold change) < -1.5 and with statistical significance ($P < 0.05$) by edgeR. The datasets generated in this study will be submitted to the Gene Expression Omnibus repository upon acceptance with the assistance of the Purdue Bioinformatics Core.

B-cell lymphoma xenograft model

NOD.Cg-Prkdcscid Il2rgtm1Wjl/SzJ (NSG) male mice, aged 10–14 weeks, were divided into groups: NK-92, CAR.19 and CAR.19-IL-27. Tumor induction was performed by injecting 2×10^4 Raji-Luc+ cells, which were previously transduced for D-luciferase expression, through the lateral tail vein. Effector cells (7×10^6) were injected via the same route on days 4, 7, 10, 12, 15 and 19. Tumor development was monitored by bioluminescence using the IVIS Lumina System (Perkin Elmer - Waltham, Massachusetts). Bioluminescence images were captured 5–10 min after intraperitoneal injection of 150 mg/kg of D-luciferin (Perkin Elmer). For peripheral blood distribution of CAR-NK cells, NSG mice were injected via lateral tail vein with 2×10^4 Raji-Luc cells and in the next day with a single dose of 7×10^6 CAR.19 or CAR.19-IL-27 cells. On days 1, 7 and 21 post-CAR-NK injections, 100 μL of blood was collected through the submandibular vein.

Analysis of CAR-NK in vivo *persistence by digital droplet PCR (ddPCR)*

For CAR transgene detection, primers and probe targeted 4-1BB and CD3ζ junction. Mouse blood gDNA was extracted using QIAmp DNA Mini Kit, digested with HindIII-HF and used for ddPCR. An amount of 22 μL ddPCR reaction included ddPCR Supermix, FAM-labeled CAR19 primer-probe assay. Droplets were generated using QX200 AutoDG Droplet Generator. DNA amplification was performed in C1000 Touch Thermal Cycler: initial denaturation at 95°C for 10 min, 40 cycles at 94°C for 30 s, 57°C for 1 min, final step at 98°C for 10 min. Droplets were analyzed in QX200 Droplet Reader, data processed with QX Manager Regulatory Edition, reported as amplicon copies per microliter.

Statistics

Comparisons between two groups with a normal distribution were conducted using the *t*-student test, and for more than two groups, one-way ANOVA followed by Tukey's post-hoc test was employed. In cases of non-normal distribution, the Mann-Whitney test was used for comparing two groups, and the Kruskal-Wallis test with Dunn's post-hoc test was utilized for comparing more than two groups. $^{*}P \leq 0.05$, $^{**}P \leq 0.01$, $^{***}P \leq 0.001$ and $^{****}P \leq 0.0001$. Statistics and graphs were made with GraphPad Prism software version 9.

Results

Generation of NK-92 cells expressing CAR.19 and CAR.19-IL-27

We constructed a lentiviral vector carrying a fourth-generation CAR with specificity for the CD19 molecule and coexpressing human IL-27. To allow for coexpression of CAR and IL-27, a self-cleaving peptide sequence (2A) was inserted between the CAR and IL-27 genes. We also generated a second-generation CAR.19 construct without IL-27 (Figure 1A) as control. Both CAR constructs were inserted into lentiviral vectors and used to transduce human NK-92 cells. This resulted in two cell populations: NK-92-CAR.19 cells and NK-92-CAR.19-IL-27 cells. To ensure a consistent and stable expression of CAR on the surface of NK-92 cells, we performed two rounds of immunomagnetic positive selection. This process resulted in a homogeneous population of CAR-expressing NK-92 cells, which maintained CAR expression even after 30 days in culture (Figure 1B,C).

After expanding NK-92 cells and variants, we characterized them for the expression of NK cell-specific markers. Our findings revealed that the expression levels of CD56, CD45, CD28, CD16, CD11a (LFA-1), CD2, NKG2D, NKp30, NKp46 and CD95 were highly comparable between the engineered CAR cells and the parental NK-92 cells (Figure S2). This observation implies that the introduction of CAR.19 or CAR.19-IL-27 had no significant impact on the expression of these markers. Although the percentage of CD56 marker was similar across NK-92 and the CAR-modified cells (Figure 2A), notably, the CD56 mean fluorescence intensity (MFI) was significantly reduced in both CAR.19 cells, with the CAR.19-IL-27 showing the most significant CD56 reduction relative to both NK-92 and CAR.19 ($P < 0.0003$) (Figure 2).

IL-27 boosts CAR.19 cell proliferation

We next performed a growth assay to determine whether production of IL-27 by the transgenic cells could impact the intrinsic viability of NK-92 cells. CAR.19-IL-27 cells exhibited a significant increase of viable cells over time, relative to CAR.19 and NK-92 cells in the presence of IL-2 (Figure 3A). However, none of the NK-92 cells sustained

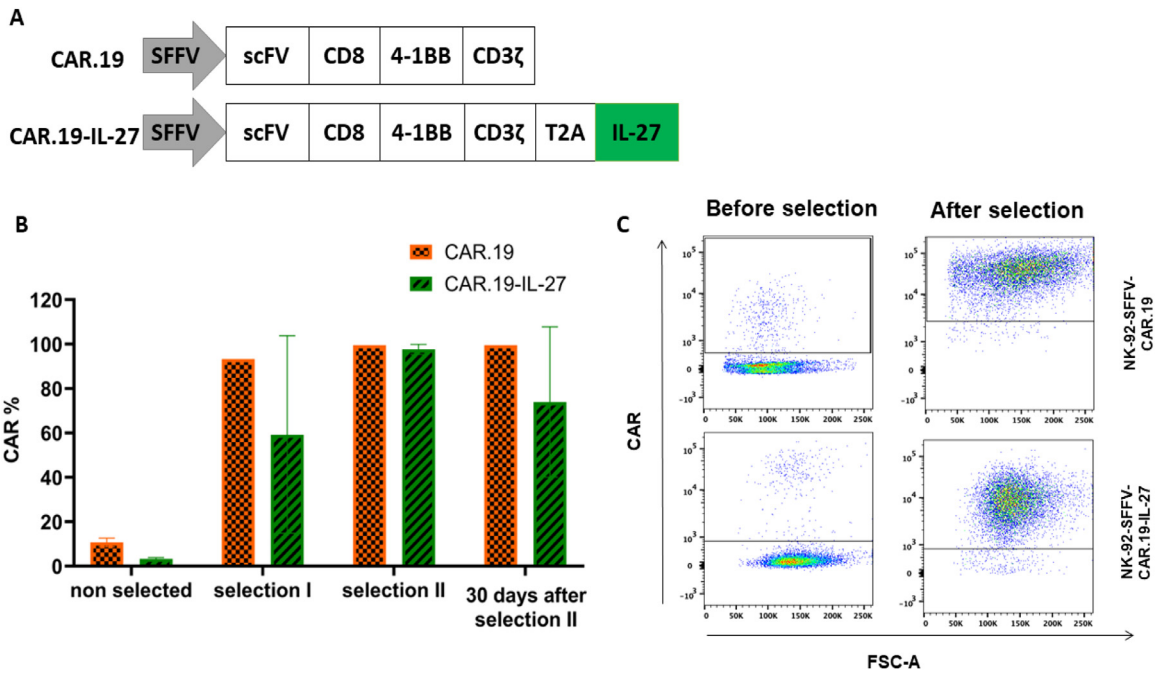

Fig. 1. Generation of CAR.19 and CAR.19-IL-27 cells. (A) CAR construct's scheme specifically targets CD19 under the regulation of the spleen focus-forming virus (SFFV) promoter. The CAR construct consists of a single-chain variable fragment (scFv), CD8 hinge and transmembrane region, 41BB costimulatory molecule, and CD3ζ signaling molecule. CAR sequence is followed by a self-cleaving peptide (T2A) and IL-27. (B) Enrichment of CAR-positive NK cells after transduction performed in two steps, cells were stably expressing CAR for over 30 days. (C) Flow cytometry analysis of CAR constructs before and after positive selection of CAR-NK cells with magnetic beads. (Color version of figure is available online.)

cell growth in the absence of IL-2 (Figure 3C). Cell viability was maintained between 80% and 95% during the 21 days of culture with IL-2 (Figure 3B) and viability drops drastically after 15 days of culture without IL-2 (Figure 3D). CAR.19-IL-27 cells were confirmed to secrete high levels of IL-27 (Figure 3E), whereas only low levels of IL-27 were detected in the supernatant of CAR.19 cells.

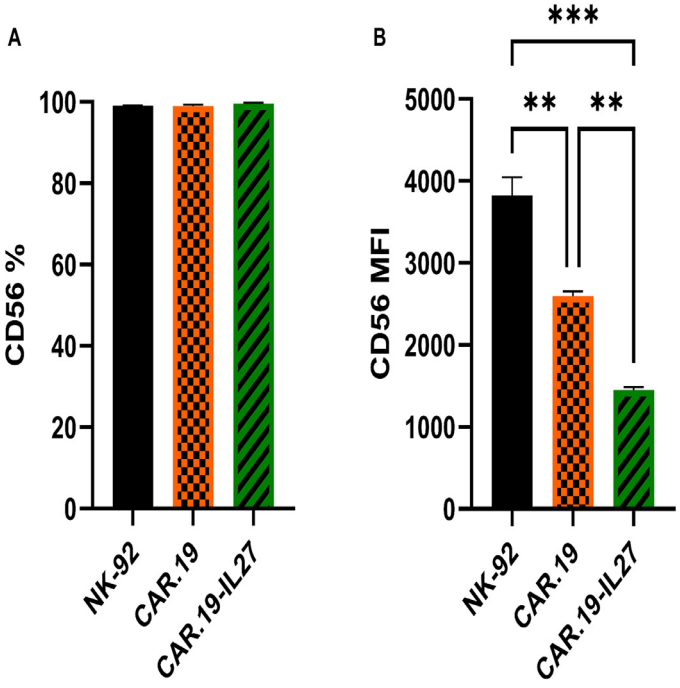

Fig. 2. Expression of CD56 on CAR.19 and CAR.19-IL-27 cells. (A) The percentage of cells positive for CD56 did not change among parental cells and constructs. (B) The MFI of CD56 decreased among the constructs, compared to parental cells, with CAR.19-IL-27 expressing the lowest amount of fluorescence. $n = 3$, means + SEM are shown. Data was evaluated by flow cytometry. One-way ANOVA statistical test was used, with multiple comparison post-test of Tukey. $P < 0.01$ (**) and $P < 0.0003$ (***). (Color version of figure is available online.)

CAR.19-IL-27 cells exhibit potent cytotoxic activity against CD19+ cell lines

We further studied how IL-27 might affect the specific cytotoxicity of CAR-NK cells against CD19+ B-cell malignancies. To model this effect, we used two CD19-positive cell lines, Raji and NALM-6. Through co-culture assays, we observed that all CD19-specific CAR NK-92 cells showed a significant increase in cytotoxicity against both NALM-6 and Raji cells, in comparison to unmodified NK-92 cells (Figure 4A). Moreover, CAR.19-IL-27 cells had even greater cytotoxicity relative to CAR.19 against target cells (Figure 4A). These results indicate the potential of IL-27 to further enhance the antitumor function of CAR.19 cells, particularly when targeting CD19+ B-cell malignancies. The observed higher cytotoxicity seems to correlate with an increase in CD107a expression (both in percentage of positive cells, Figure 4B; and intensity of expression, Figure 4C). Also, results indicated an increase in the levels of IFN-γ (Figure 4D) and a reduction in TNF-α relative to CAR.19 (Figure 4E). Conversely, no discernible distinctions were observed in the expression of granzymes A and B, perforin, IL-8, IL-10 and IL-18, suggesting the changes might not be CAR-dependent (Figure S3).

Differential gene expression analyses unveiled distinct pathways that are upregulated in IL-27-expressing cells

Next, we performed RNA sequencing (RNA-seq) analysis to characterize gene transcription changes associated with IL-27 expression in CAR.19-IL-27 cells relative to CAR.19, in co-culture/stimulated with Raji cells. The volcano plot shows the differentially expressed genes (DEGs) from each sample, with CAR.19-IL-27 cells having 693 upregulated genes and 674 downregulated genes (Figure 5A). A gene heatmap shows distinct clusters of up and downregulated genes among the samples (Figure 5B). Of all the DEGs, GO enrichment analysis revealed that for *biological processes*, most genes related to signal

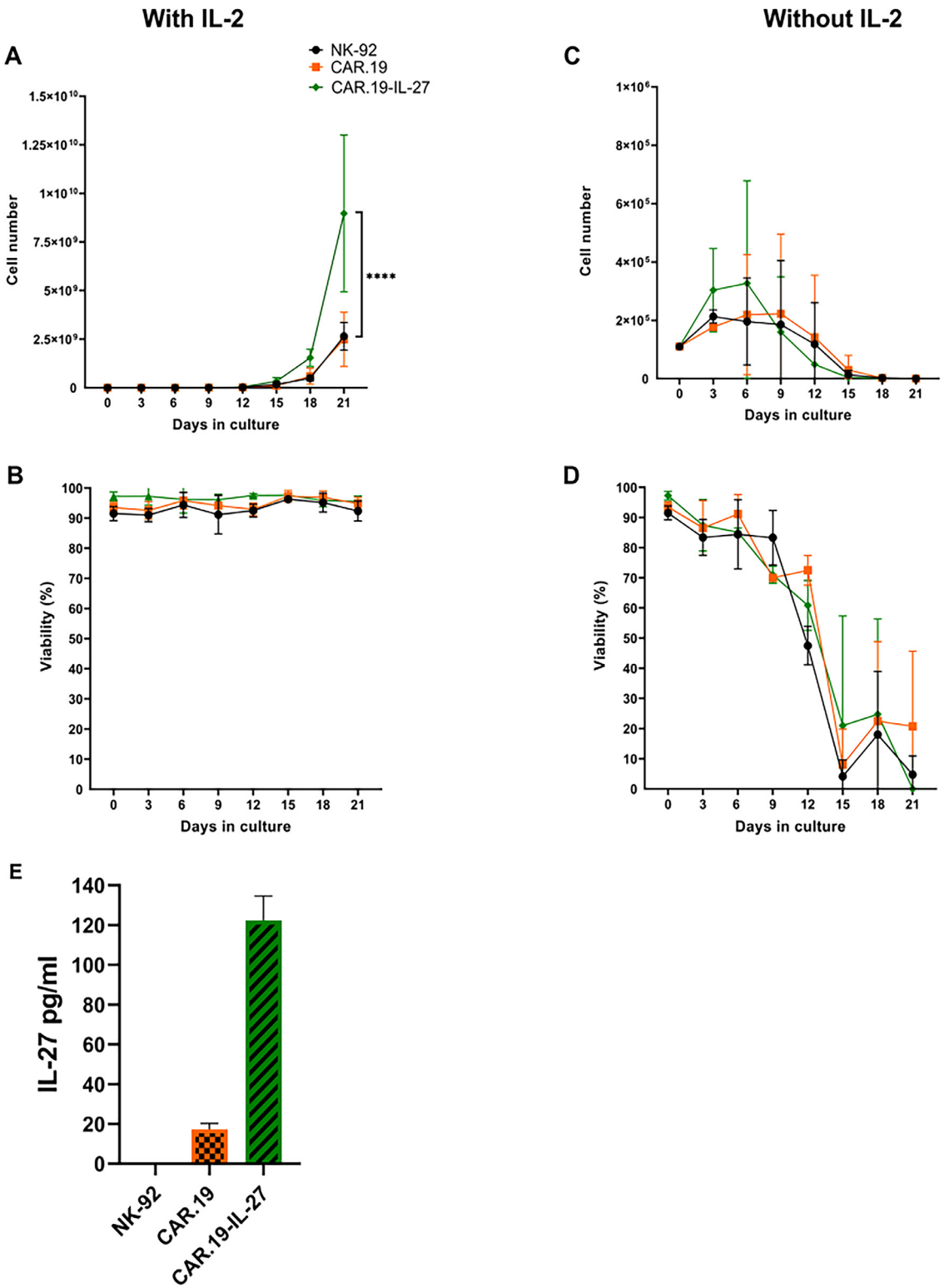

Fig. 3. Enhanced Proliferation of CAR.19-IL-27 cells with exogenous IL-2 supplementation. Cells were cultured either in presence (A and B), or absence (C and D) of IL-2 (500 UI/mL). Cell culture was followed over 21 days. $n = 4$, means + SEM are shown. (E) Quantification of soluble IL-27 in supernatant of NK-92 cell culture by Luminex ($n = 2$). Two-way ANOVA statistical test, Tukey's postmultiple comparison posttest. $^{****}P < 0.0001$. (Color version of figure is available online.)

transduction; for *cellular components*, most genes related to the membrane, and for *molecular function*, to protein binding (Figure 5C). Some of the genes common to these processes that were upregulated in CAR.19-IL-27 cells included *NCR2*, *MRAS* and *TRAF4* (log2(fc) = 3.43, 3,51, 1,78, respectively), suggesting increased activation and proliferation of these cells. These results demonstrate the role of IL-27 in modifying the transcriptome profile of CAR.19 cells.

We then performed enrichment analysis using the DEGs that were upregulated in CAR.19-IL-27 cells relative to CAR.19. *Metascape* [18] analysis revealed that cytokine-related pathways were the most upregulated, and that genes related to the MAPK cascade were also

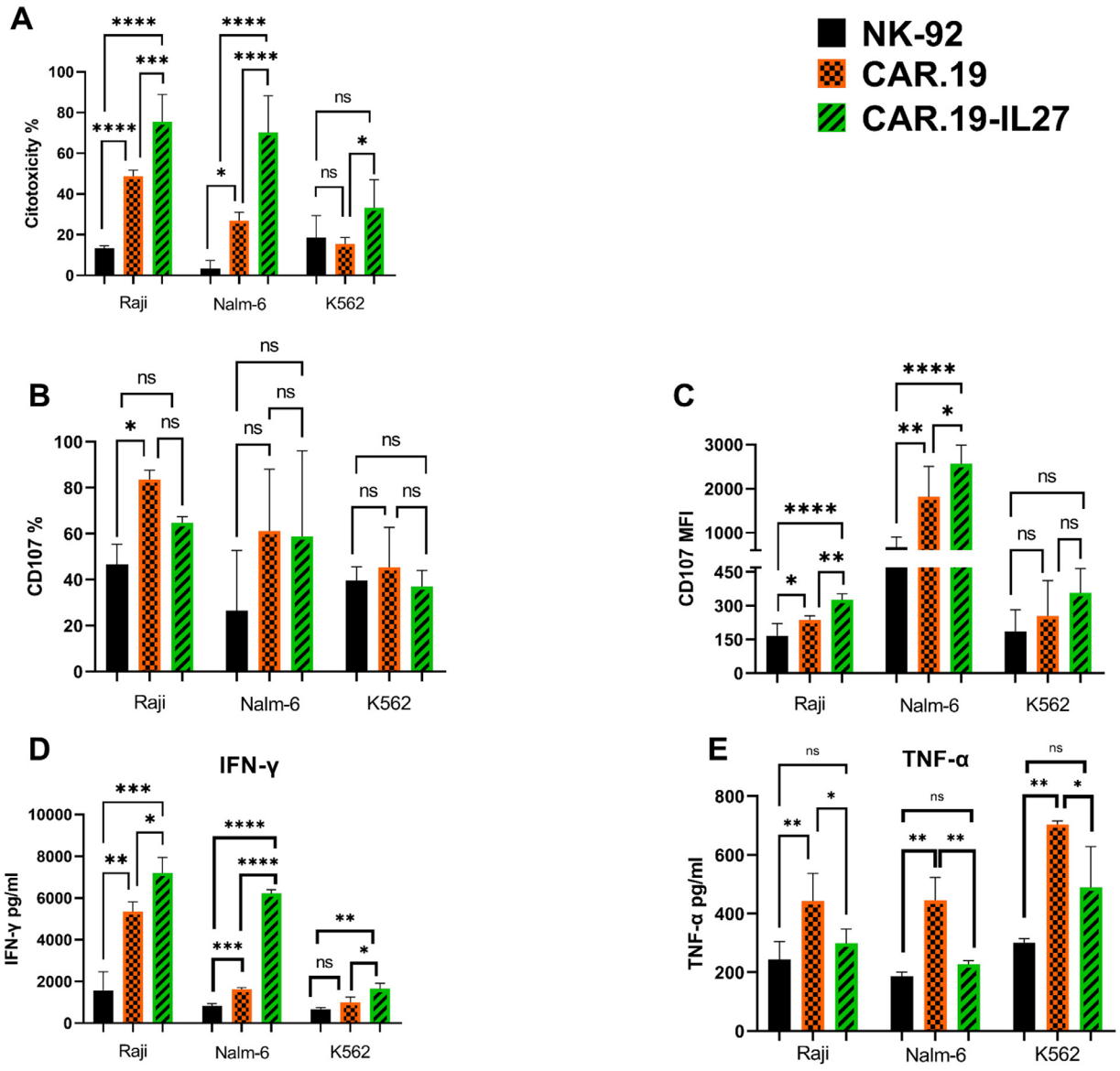

Fig. 4. Cytotoxic profile of NK-92, CAR.19 and CAR.19-IL-27 cells. (A) Cytotoxicity of NK-92, CAR.19 and CAR.19-IL-27 cells co-cultured in 2:1 (E:T) ratio for 5 h with CD19+ tumor cell lines Raji, NALM-6; and CD19-K562. (B) Percentage of CD107a+ cells and (C) MFI of the positive CD107a cells assessed by flow cytometry. (D) INF-γ and (E) TNF-α secreted by NK-92, CAR.19 and CAR.19-IL-27 cells, assessed by ELISA. n = 3, means + SEM are shown. One-way ANOVA statistical test was used, with multiple comparison post-test of Tukey. The following P values were considered significant: $P < 0.05$ (*), $P < 0.01$ (**); $P < 0.0003$ (***) and $P < 0.0001$ (****). (Color version of figure is available online.)

upregulated (Figure 5D). The same set of genes was then analyzed using *gProfiler* [19], and congruent with the *Metascape* analysis, genes related to MAPK, ERK1/2 and the JNK cascades, were significantly upregulated (Table 1). Gene set enrichment analysis showed that significantly upregulated enriched pathways/processes included *positive regulation of the JNK cascade* (Figure 5E), and positive regulation of the p38 MAPK cascade (not shown) (NES = 1.72, P value = 0.002, FDR = 0.047). With the same dataset, we evaluated the transcripts detected for several genes that are of biological relevance for NK cells, and that were upregulated in CAR.19-IL-27, which included *IL-27, IL-2Ra, IL-15Ra, IRF5, FAS, NCR2* (NKp44), *NCR3* (NKp30), *GZMB, GZMM, CXCL8* and *CXCR4* (Figure 5F), noting several fold-change upregulations >2.0 for *IL-27, IL2RA, IRF5, FAS, NCR2, CXCL8* and *CXCR4*.

Validation of data from RNAseq

To validate the RNAseq findings, we conducted FACS analysis to assess the phosphorylation of the ERK pathway, belonging to the MAPK signaling pathway family, identified in the RNAseq enrichment analysis. NK-92 and NK-92-CAR cells were stimulated with Raji cells for 30 min at 37°C, in a 1:1 ratio. The results revealed that in CAR.19-IL-27, there was a significantly more pronounced phosphorylation of ERK1/2 compared to CAR.19 and NK-92 cells, indicating a faster and more robust activation of this pathway (Figure 6A). Example FACS dot plots of nonstimulated vs stimulated cells are shown in Figure S4. Furthermore, the gene coding for NKp44, *NCR2*, showed upregulation in the RNAseq analysis. To corroborate this, we examined NKp44 protein expression via FACS under the same conditions as the RNAseq experiment. Notably, we observed increased expression in stimulated CAR-19.IL-27 cells compared to CAR.19 and NK-92 cells (Figure 6B).

Given the apoptotic processes highlighted in the GO enrichment analysis (Figure 5C,D), we investigated whether NK-92 cells underwent apoptosis upon activation. The analysis showed a difference in apoptotic cells only between CAR.19 and NK-92 cells (Figure 6C). However, no significant differences were observed between CAR.19 and CAR.19.IL-27, indicating changes related to apoptotic processes happened only at transcriptional levels. Nevertheless, we confirmed

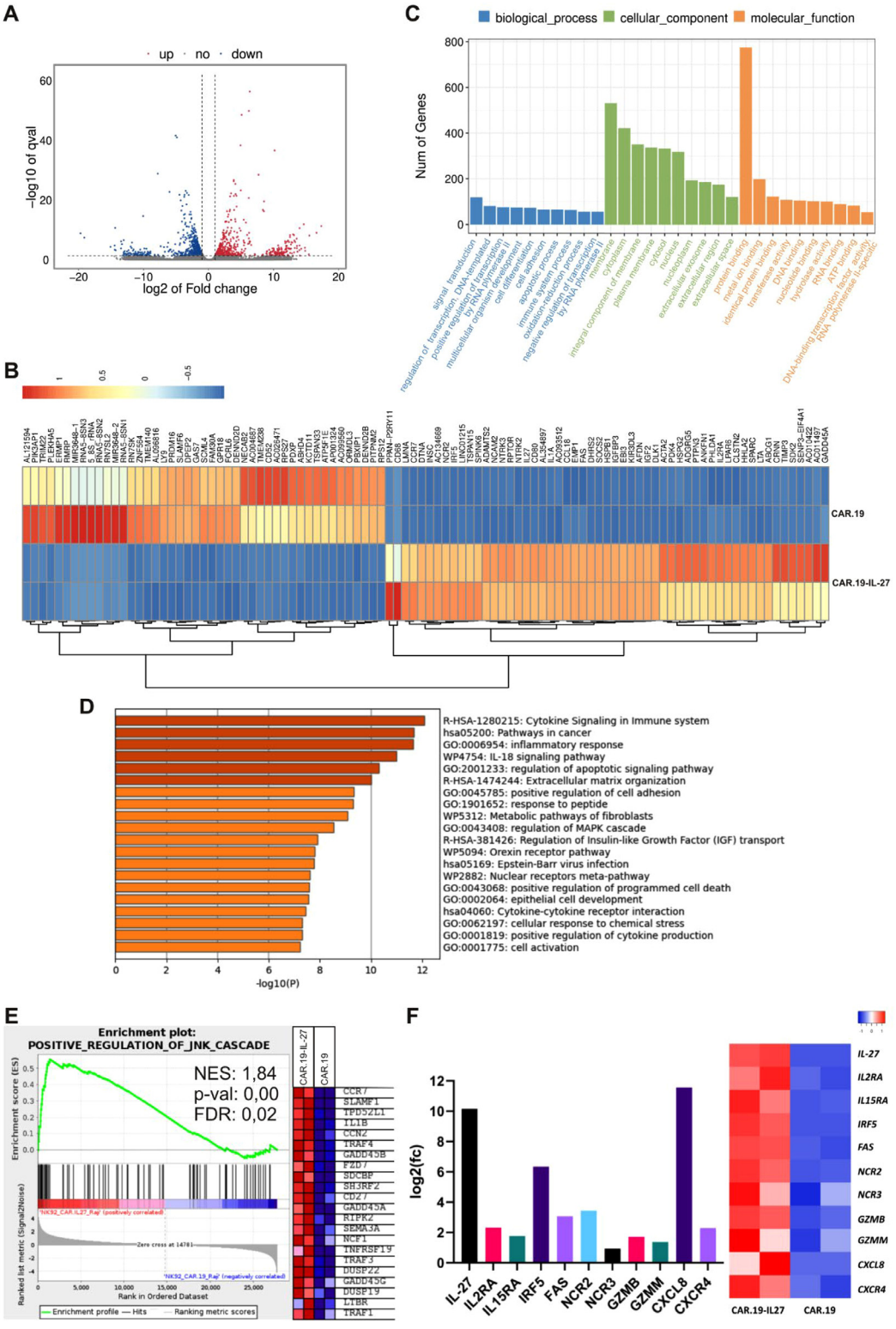

Fig. 5. Systemic transcriptomic analysis of activated CAR.19 and CAR.19-IL-27 cells. (A) Volcano plot of differentially expressed genes in CAR.19-IL-27 compared to CAR.19. (B) Heatmap of differentially expressed genes, showing distinct clusters among CAR.19 (top) and CAR.19-IL-27 (bottom) replicates. (C) GO enrichment analysis (biological process, molecular function and cellular component) of codifferential expression genes in CAR.19-IL-27. Highly significant enriched gene sets are shown in (D) Bar graph of enriched terms across differentially upregulated genes in CAR.19-IL-27 cells, obtained using Metascape. (E) GSEA of upregulated *positive regulation of JNK cascade* pathway. (F) Genes of biological relevance for NK cells that were upregulated in stimulated CAR.19-IL-27 cells. log2(fc) of the mean of the replicates in each group (left). Heatmap of FPKM of each replicate in CAR.19-IL-27 and in CAR.19 cells (right). (Color version of figure is available online.)

Table 1
gProfiler GO enrichment analysis of upregulated DEGs in CAR.19-IL-27 compared to CAR.19, showing the main pathways and genes.

Term	Description	Genes	Adj. *P* value
GO:0000165	MAPK cascade	NTRK3,IGFBP3,PTPN3,AC134669,IGF2,FAS,NTRK2,TIMP3,CCR7,ACTA2,IL1A,GADD45A,CCL18,AC093512, CSF1R,SLAMF1,CD36,FN1,DAB2,ICAM1,MAGED1,PRDX2,TRAF4,CEACAM1,SFRP1,SPRED2,CX3CL1, PIK3R6,JUN,CDH2,SLC30A10,GADD45B,TNFRSF19,MDFIC,BMP4,PRKCD,MYC,PRKCE,ROBO1,TGFBR1, MFHAS1,VRK2,TPD52L1,RIPK2,PTPRR,AL365181,GLIPR2,RGS2	0.00001
GO:0043410	positive regulation of MAPK cascade	NTRK3,IGFBP3,IGF2,NTRK2,CCR7,ACTA2,IL1A,GADD45A,CCL18,AC093512,CSF1R,SLAMF1,CD36,ICAM1, MAGED1,PRDX2,TRAF4,CX3CL1,PIK3R6,JUN,CDH2,SLC30A10,GADD45B,TNFRSF19,BMP4,PRKCE, ROBO1,TGFBR1,MFHAS1,TPD52L1,RIPK2,AL365181,GLIPR2	0.00009
GO:0070371	ERK1 and ERK2 cascade	TIMP3,CCR7,ACTA2,IL1A,CCL18,CSF1R,SLAMF1,CD36,FN1,DAB2,ICAM1,CEACAM1,SPRED2,CX3CL1,JUN, SLC30A10,BMP4,MYC,MFHAS1,RIPK2,PTPRR,AL365181,GLIPR2	0.001
GO:0007254	JNK cascade	CCR7,IL1A,GADD45A,AC093512,SLAMF1,TRAF4,SFRP1,GADD45B,TNFRSF19,MDFIC,MFHAS1,TPD52L1, RIPK2	0.01
GO:0046330	positive regulation of JNK cascade	CCR7,IL1A,GADD45A,AC093512,SLAMF1,TRAF4,GADD45B,TNFRSF19,MFHAS1,TPD52L1,RIPK2	0.001

the heightened signaling of the ERK1/2 pathway and NKp44 expression in CAR.19-IL-27, at both RNA and protein levels.

Incorporating IL-27 into CAR.19 NK-92 cells enhance in vivo *cytotoxic function against murine B-cell lymphoma xenograft model*

We conducted an assessment of the antilymphoma activity of CAR.19-IL-27 cells in a Raji xenograft immunodeficient mouse model. Initially, mice were intravenously infused with Raji-Luc+ cell line (D0) followed by six infusions of either CAR.19-IL-27, CAR.19 or parental NK-92 cells on days 4, 7, 10, 12, 15 and 19, at specific cell concentrations (2×10^4/mouse for Raji-Luc+ and 7×10^6/mouse for NK cells) (Figure 7A). The tumor growth was monitored over time by measuring bioluminescence.

As expected, mice treated with control NK-92 cells exhibited a rapid increase in bioluminescence, indicative of tumor progression. In contrast, the mice receiving CAR.19-IL-27 cells demonstrated reduced rate of tumor growth in most animals from day 8 to day 21 measurements (Figure 7B–D). This suggests that adding IL-27 in CAR.19 cells resulted in a superior antitumor activity against lymphoma cells in the *in vivo* setting relative to NK-92 cells.

As demonstrated earlier, the secretion of IL-27 by CAR.19-IL-27 enhanced the proliferative capacity of these cells *in vitro*. To assess the impact of IL-27 on the survival of CAR-NK-92 cells *in vivo*, we evaluated the presence of CAR sequence persistence in the peripheral blood of Raji-Luc+ xenografted mice over 21 days. On day −1, mice were intravenously injected with tumor cells followed by, on day 0, a single dose of CAR.19 or CAR.19-IL-27 cells. As presumed, one day following CAR-NK injection, CAR sequence was detectable in the bloodstream of mice, however, by the 7th- and 20th-day following CAR-NK injection, the levels of CAR.19 or CAR.19-IL-27 copies detected did not differ from the untreated mice control group (Figure 7E). Overall, these results indicate that CAR-NK-92 cells have limited persistence *in vivo* and that incorporating IL-27 does not affect this characteristic.

These findings demonstrate the potential of IL-27 as a valuable addition for enhancing the therapeutic efficacy of NK cell-based immunotherapies for lymphoma treatment.

Discussion

The remarkable success of CAR-T cell therapy trials has resulted in FDA approval of six CAR-T cell products for the treatment of hematologic cancers [20]. However, the personalized nature of CAR-T cell therapy and the potential for severe toxicities remain significant challenges, acting as barriers to treating a broader spectrum of patients. Consequently, CAR-NK cells have emerged as a promising alternative allogeneic strategy, presenting a more favorable safety profile and inherent antitumor potential. Early studies have shown encouraging efficacy of CAR-NK cells in clinical applications [3,21,22]. However, CAR-NK cells have not exhibited an impressive clinical benefit when compared to CAR-T cells. This might be partly attributed to the challenges of NK cells' limited ability to expand and maintain cytotoxicity *in vivo*. Nevertheless, combining cytokines to CAR-NK cells has shown promise in enhancing their response against

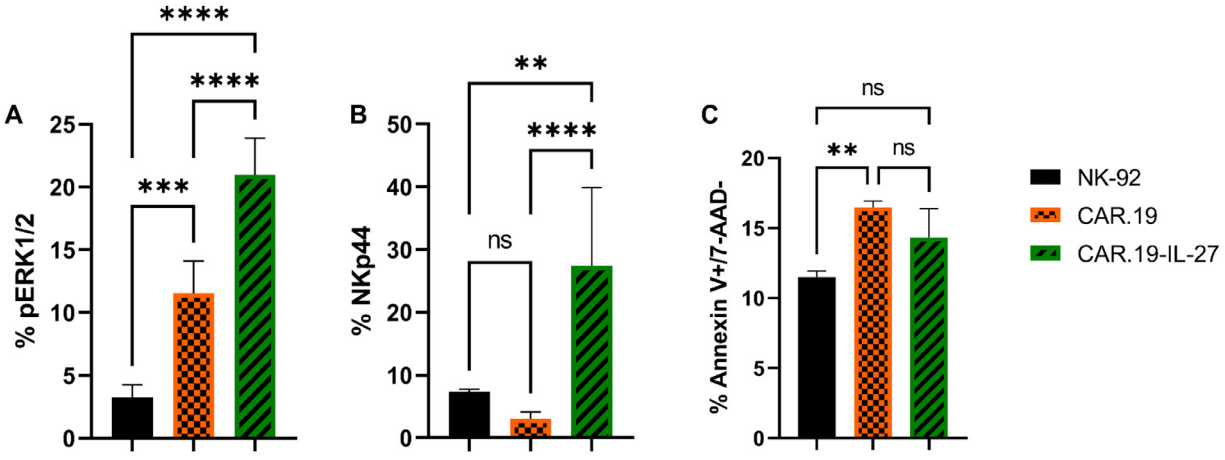

Fig. 6. Validation of frequent data on RNAseq. (A) NK-92 and NK-92-CAR cells were stimulated with Raji cells, for 30 min at 37°C, at a 1:1 ratio. Results show phosphorylated ERK1/2, of the MAPK signaling pathway. (B) NKp44 expression after target cell stimulation and (C) apoptotic cells considering annexin V+/7-AAD-cells (live, apoptotic cells). All results were analyzed by FACS from live CD56+ gated cells. For B and C cells were stimulated in the same conditions as the RNAseq (10:1 E:T, 24 h). $n = 3$, means + SEM are shown. One-way ANOVA statistical test was used, with multiple comparison post-test of Tukey. The following P values were considered significant: $P < 0.01$ (**); $P < 0.0003$ (***) and $P < 0.0001$ (****). (Color version of figure is available online.)

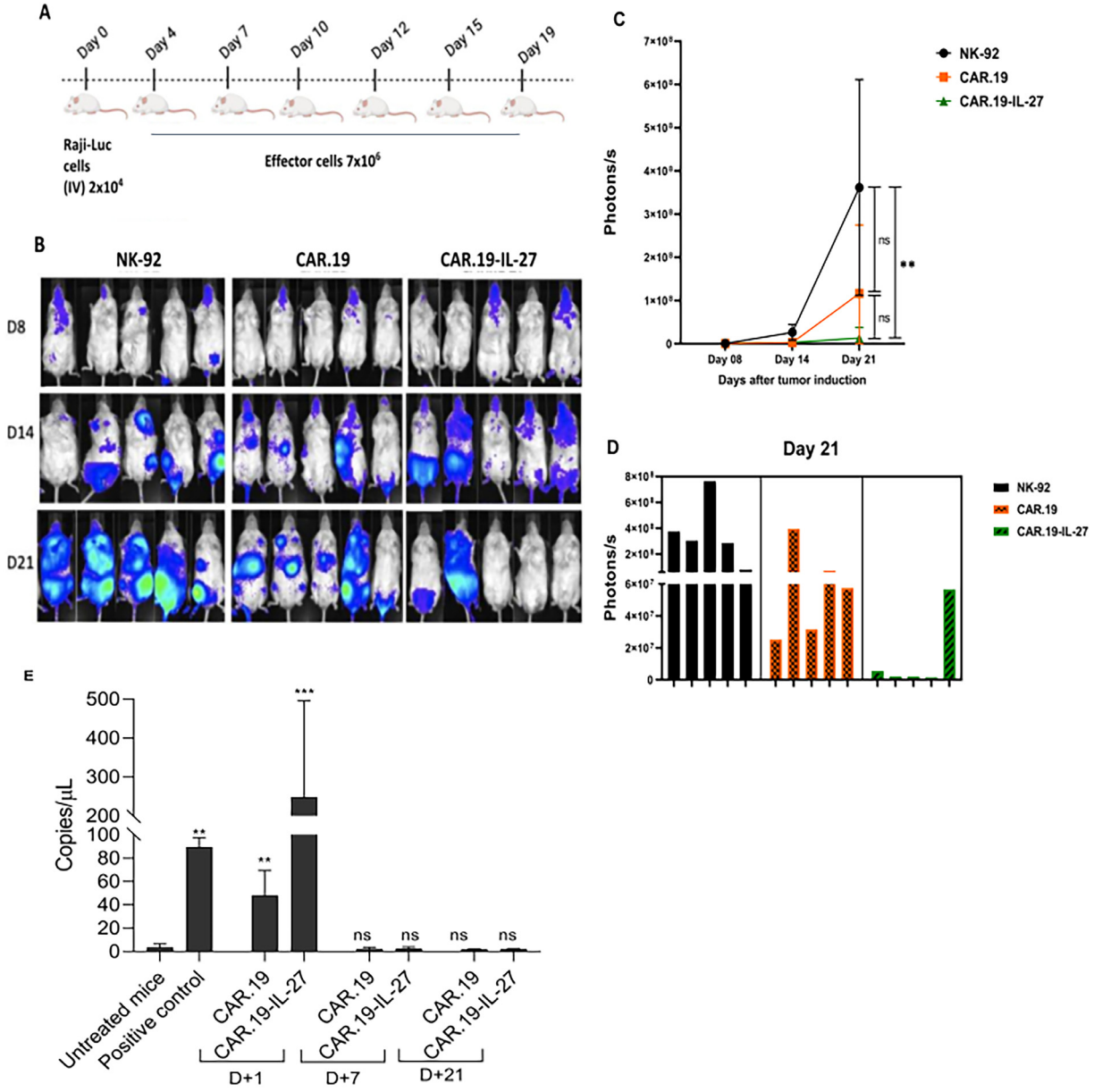

Fig. 7. CAR.19-IL-27 cells exhibit potent *in vivo* antitumor potential. (A) Scheme of an *in vivo* study demonstrating the antitumor activity of transduced CAR NK cells in a xenogeneic NSG mouse model of disseminated human B-cell malignancy. NSG mice were intravenously injected with 2×10^4 Raji-Luc lymphoma cells. On days 4, 7, 10, 12, 15 and 19, animals were treated by intravenous injection of 7×10^6 effector cells. (B) Lymphoma development was monitored by *in vivo* bioluminescence imaging. Images were taken on days 8, 14 and 21. (C) Bioluminescence intensity was quantified, and data are shown as mean ± SEM, $n = 5$. Kruskal-Wallis test on day 21, $P < 0.01$ (**). (D) Bioluminescence of individual mice shown on day 21. (E) Persistence of CAR-NK cells in peripheral blood evaluated by ddPCR. NSG mice were intravenously injected with Raji-Luc cells on day −1 and received on day 0 CAR.19 or CAR.19-IL-27 cells. On days 1, 7 and 21, blood samples were collected, and the extracted DNA was analyzed for CAR sequence copies. $n = 2$ for "untreated mice" and "CAR.19," and $n = 3$ for "CAR.19-IL-27," means + SEM are shown. $P < 0.01$ (**); $P < 0.01$ (**); $P < 0.0003$ (***) and $P < 0.0001$ (****). ns, nonsignificative. (Color version of figure is available online.)

cancer cells, offering a potential avenue for improving their therapeutic efficacy.

Studies have reported that IL-27 possesses potent anti-tumor activity against various tumor models, through multiple mechanisms which include the activation of NK cells [9,15]. There is also evidence demonstrating IL-27's direct anti-tumor effects in hematologic malignancies by inducing apoptosis in leukemic cells and inhibiting proliferation, particularly in pediatric B acute lymphoblastic leukemia [23,24]. Emerging immunotherapeutic strategies encompass strengthening the function of endogenous NK cells through cytokine stimulation, including IL-2, IL-15, IL-18, and the adoptive transfer of CAR-NK cells engineered to express these cytokines [25]. Notably, there is currently no existing study that describes the effects of fourth-generation CAR-expressing IL-27 on NK cells. Therefore, our research investigates, both *in vitro* and *in vivo*, the potential impact of IL-27 on NK cell activity against B malignancies.

In this study, we demonstrated that IL-27 could stimulate NK cell proliferation in the presence of IL-2. However, IL-27 alone did not induce cell proliferation, suggesting that by itself, it is not sufficient to trigger this process, but rather plays a role in enhancing it. This result is not surprising, given that the NK-92 cell line is typically dependent on IL-2 for proliferating [26]. Nevertheless, IL-27 facilitated remarkable cell growth, achieving an increase in viable NK cells of over 30-fold in just 21 days of culture. Recently, we demonstrated that CAR-expressing IL15/IL-15R can effectively replace IL-2 in the NK-92 expansion process [25], an effect not observed with the present design of the CAR-expressing IL-27.

In addition to the notable increment in cell growth, incorporating IL-27 into CAR-NK cells was shown to augment their cytotoxicity against CD19+ cell lines. This enhancement led to increased secretion of IFN-γ and elevated expression of CD107a on the surface of CAR.19-IL-27 cells. Interestingly, no increase in TNF-α was observed, consistent with a previous related study [9]. The increased expression of CD107a on the NK cell surface is typically a sign of degranulation [27], which supports the idea that perforins and granzymes play a role in the improved cytotoxicity of CAR.19-IL-27 against CD19+ cells. This finding highlights a high potential for CAR-NK cells with added IL-27 to enhance anti-tumor responses through granule-mediated mechanisms. Prior research has demonstrated that both endogenous IL-27 [28–30], and exogenous IL-27 have a positive influence on the antitumor activity of T cells [31,32] and NK cells [9,33].

To have a better understanding of molecular pathways modulated by IL-27 expression, we conducted RNA sequencing in activated NK-92-CAR.19 cells. Our bioinformatics analyses revealed clear distinctions in gene expression profiles between CAR.19-IL-27 and CAR.19 cells. Notably, our data demonstrated that IL-27 initiated a sequence of intracellular processes that culminated in the upregulation of genes related to the MAPK signaling pathway, encompassing ERK1/2, p38 and JNK. Our results are supported by previous studies which showed that IL-27 activates MAPK-related pathways [34,35]. As aforementioned, our results showed increased proliferation and IFN-γ secretion of CAR.19-IL-27 cells. Previous studies have shown that IL-27 is able to increase proliferation of leukemic cell lines through ERK1/2 signaling [35]; and that IL-27 stimulates IFN-γ secretion through, among others, MEK1/2 and JNK signaling in primary NK cells [9]. Our RNAseq showed upregulation of target genes downstream of MAPK-cascade that increase cell proliferation and survival, such as c-JUN, c-MYC (Table 1) [36] and FAS (Figure 5) [37]; and type I and II interferons, such as IRF5 (Figure 5), and ICAM-1 (Table 1) [38,39]. In combination, these results suggest incorporating IL-27 into CAR.19 NK cells can increase cell proliferation and promote IFN-γ production, potentially through MAPK-related pathways.

Our RNAseq results also demonstrated that IL-27 upregulated genes of biological relevance to NK cells. As is the case with the activating receptors NKp30 and NKp44, belonging to the family of natural cytotoxicity receptors, which initiate tumor target recognition and increase activation of NK cells [40]. Granzymes that are abundantly expressed on NK cells were also upregulated by IL-27, such as Granzyme B and M. Granzyme B-dependent killing occurs by activating the target cell's intrinsic cell death proteases and caspases, triggering caspase-mediated degradation of numerous cellular protein substrates, leading to cell apoptosis [41]. Granzyme-M on the other hand, promotes tumor cell death by inducing cytoskeleton disorganization, leading to cell death [42]. Signaling through the IL-2 and IL-15 receptors plays a vital role in various aspects of NK cell activation by these cytokines, notably proliferation, cytolytic activity and cytokine production [43]. Here we show that CAR.19-IL-27 cells have increased expression of IL-2Rα and IL-15Rα, indicating a potential mechanistic role of these cytokines.

Trafficking of NK cells to the bone marrow and lymphoid tissues, where hematological cancers usually develop and reside, depends on chemotaxis. CCR7 directs NK cells to lymphoid tissues and is responsible for homing of these cells in the lymph nodes [44]. Recent studies have shown that increased expression of CXCR4 in CAR-NK cells leads to a strong response against target cells, and increases homing of NK cells to the bone marrow [45,46]. Homing of NK cells to the bone marrow has also been associated with better leukemia control and remission in patients who received NK-cell therapy [47]. Our RNA-seq results showed that CCR7 (Table 1) and CXCR4 (Figure 5) genes were upregulated in CAR.19-IL-27 cells, suggesting a potential role for IL-27 in enhancing homing of NK to tumors. There is also evidence that IL-27 acts as an agonist of 41BB signaling, which is present in our CAR construct, and could indicate its ability to enhance signaling through this pathway [48,49].

To verify whether the positive *in vitro* outcomes observed with CARs expressing IL-27 hold preclinical therapeutic efficacy, NK-92, CAR.19 and CAR.19-IL-27 were injected in a xenograft NSG mouse model using CD19+ Raji cells. Previously, neither parental NK-92 cells nor NK-92-CAR cells have shown significant proliferation *in vivo* or sustained engraftment in NSG mice [50–52]. Therefore, we employed a systemic injection approach for delivery of NK-92 cells, administering repeated intravenous injections. Notably, treatment with parental NK-92 had minimal effects, leading to an inability to control the growth of disseminated lymphoma in various organs. In contrast, mice treated with CAR.19 and CAR.19-IL-27 exhibited delayed growth of Raji cells, indicating some degree of control over tumor progression. CAR.19-IL-27 cells demonstrated enhanced capability in controlling tumor growth in most animals.

In summary, our findings suggest that integrating IL-27 into CAR.19 NK-92 cells enhance their inherent proliferative ability. Furthermore, IL-27 improves *in vitro* antitumor activity, characterized by heightened cytotoxicity of NK-92-CAR.19 against target cell lines. This effect is mediated by increased expression of degranulation markers and IFN-γ, potentially facilitated through MAPK-related pathways. Moreover, our *in vivo* experiments illustrate the efficacy of IL-27 in enhancing the control of tumor cells through NK-92-CAR.19 expression. This study underscores the potential of IL-27 as a viable strategy to augment the antitumor capacity of CAR-NK cells, presenting a promising therapeutic avenue for cancer treatment through adoptive cell transfer.

Funding

This study was financially supported by FAPESP #2020/08279-8, #2019/25309-0, 2013/08135-2, #2008/578773; NPOP-Nutec2020/07055-9 and by CNPq t#573754-2008-0, #442484/2020-8) and CAPES—Finance Code 001 and grant #88887.817043/2023-00.

Author Contributions

AFBB and RNS have equally contributed to acquisition, analysis and interpretation of data. MCT and JTCA contributed with data acquisition. Drafting or revising the manuscript: AFBB, RNS, MCT, HDMG, KCRM, MLF, VPC. MHS, SCGL and LEBS contributed with the additional *in vivo*-related data acquisition and drafting. All authors have approved the final article.

Ethics Statements

Ethical approval was not required for the studies on humans in accordance with the local legislation and institutional requirements because only commercially available established cell lines were used. The animal study was approved by CEUA government committee in Brazil (124/2017).

Declaration of competing interest

The authors declare that they have no known competing financial interests or personal relationships that could have appeared to influence the work reported in this article.

Acknowledgments

We thank Sima Ebrahimabadi, Dayanne Schmidt and Mara Elisama da Silva for their valuable contributions, and Sandra Navarro for the artwork.

Supplementary materials

Supplementary material associated with this article can be found in the online version at doi:10.1016/j.jcyt.2024.06.001.

References

[1] Lu H, Zhao X, Li Z, Hu Y, Wang H. From CAR-T cells to CAR-NK cells: a developing immunotherapy method for hematological malignancies. Front Oncol 2021;11:720501. | PMID: 34422667; PMCID: PMC8377427.

[2] Klingemann H. Are natural killer cells superior CAR drivers? Oncoimmunology 2014;3:e28147. | PMID: 25340009; PMCID: PMC4203506.

[3] Liu E, Marin D, Banerjee P, Macapinlac HA, Thompson P, Basar R, et al. Use of CAR-transduced natural killer cells in CD19-positive lymphoid tumors. N Engl J Med 2020;382:545–53. | PMID: 32023374; PMCID: PMC7101242.

[4] Hunter BD, Jacobson CA. CAR T-cell associated neurotoxicity: mechanisms, clinicopathologic correlates, and future directions. J Natl Cancer Inst 2019;111:646–54. | PMID: 30753567.

[5] Long EO, Kim HS, Liu D, Peterson ME, Rajagopalan S. Controlling NK cell responses: integration of signals for activation and inhibition. Annu Rev Immunol 2013;31:227–58. https://doi.org/10.1146/annurev-immunol-020711-075005. 10.1146/annurev-immunol-020711−75005| PMID: 23516982; PMCID: PMC3868343.

[6] Mehta RS, Rezvani K. Chimeric antigen receptor expressing natural killer cells for the immunotherapy of cancer. Front Immunol 2018;9:283. | PMID: 29497427; PMCID: PMC5818392.

[7] Zhang L, Meng Y, Feng X, Han Z. CAR-NK cells for cancer immunotherapy: from bench to bedside. Biomark Res 2022;10:12.

[8] Zwirner NW, Ziblat A. Regulation of NK cell activation and effector functions by the IL-12 family of cytokines: the case of IL-27. Front Immunol 2017;8:25. | PMID: 28154569; PMCID: PMC5243847.

[9] Ziblat A, Domaica CI, Spallanzani RG, Iraolagoitia XLR, Rossi LE, Avila DE, et al. IL-27 stimulates human NK-cell effector functions and primes NK cells for IL-18 responsiveness. Eur J Immunol 2015;45:192–202.

[10] Choi YH, Lim EJ, Kim SW, Moon YW, Park KS, An H-J. IL-27 enhances IL-15/IL-18-mediated activation of human natural killer cells. J Immunother Cancer 2019;7:168. | PMID: 31277710; PMCID: PMC6612093.

[11] Murugaiyan G, Saha B. IL-27 in tumor immunity and immunotherapy. Trends Mol Med 2013;19:108–16. | PMID: 23306374.

[12] Cocco C, Di Carlo E, Zupo S, Canale S, Zorzoli A, Ribatti D, et al. Complementary IL-23 and IL-27 anti-tumor activities cause strong inhibition of human follicular and diffuse large B-cell lymphoma growth in vivo. Leukemia 2012;26:1365–74.

[13] Cheng J, Myers TG, Levinger C, Kumar P, Kumar J, Goshu BA, et al. IL-27 induces IFN/STAT1-dependent genes and enhances function of TIGIT+ HIVGag-specific T cells. iScience 2022;25:103588. | PMID: 35005538.

[14] Stumhofer JS, Silver JS, Laurence A, Porrett PM, Harris TH, Turka LA, et al. Interleukins 27 and 6 induce STAT3-mediated T cell production of interleukin 10. Nat Immunol 2007;8:1363–71.

[15] Hisada M, Kamiya S, Fujita K, Belladonna ML, Aoki T, Koyanagi Y, et al. Potent anti-tumor activity of interleukin-27. Cancer Res 2004;64:1152–6. | PMID: 14871851.

[16] Liu J-Q, Zhang C, Zhang X, Yan J, Zeng C, Talebian F, et al. Intratumoral delivery of IL-12 and IL-27 mRNA using lipid nanoparticles for cancer immunotherapy. J Control Release 2022;345:306–13. | PMID: 35301053; PMCID: PMC9133152.

[17] Figueiredo ML, Letteri R, Chan-Seng D, Kumar S, Rivera-Cruz CM, Emrick TS. Reengineering tumor microenvironment with sequential interleukin delivery. Bioengineering (Basel) 2021;8:90. | PMID: 34209203; PMCID: PMC8301035.

[18] Zhou Y, Zhou B, Pache L, Chang M, Khodabakhshi AH, Tanaseichuk O, et al. Metascape provides a biologist-oriented resource for the analysis of systems-level datasets. Nat Commun 2019;10:1523. | PMID: 30944313; PMCID: PMC6447622.

[19] Kolberg L, Raudvere U, Kuzmin I, Adler P, Vilo J, Peterson H. g:Profiler-interoperable web service for functional enrichment analysis and gene identifier mapping (2023 update). Nucleic Acids Res 2023;51:W207–12. | PMID: 37144459; PMCID: PMC10320099.

[20] FDA. Approved Cellular and Gene Therapy Products, 2023. Available at: https://www.fda.gov/vaccines-blood-biologics/cellular-gene-therapy-products/approved-cellular-and-gene-therapy-products (Accessed December 3, 2023).

[21] Biederstädt A, Rezvani K. Engineering the next generation of CAR-NK immunotherapies. Int J Hematol 2021;114:554–71. | PMID: 34453686; PMCID: PMC8397867.

[22] Oelsner S, Friede ME, Zhang C, Wagner J, Badura S, Bader P, et al. Continuously expanding CAR NK-92 cells display selective cytotoxicity against B-cell leukemia and lymphoma. Cytotherapy 2017;19:235–49. | PMID: 27887866.

[23] Cocco C, Giuliani N, Di Carlo E, Ognio E, Storti P, Abeltino M, et al. Interleukin-27 acts as multifunctional antitumor agent in multiple myeloma. Clin Cancer Res 2010;16:4188–97.

[24] Cocco C, Pistoia V, Airoldi I. Anti-leukemic properties of IL-12, IL-23 and IL-27: differences and similarities in the control of pediatric B acute lymphoblastic leukemia. Crit Rev Oncol Hematol 2012;83:310–8.

[25] Silvestre RN, Eitler J, de Azevedo JTC, Tirapelle MC, Fantacini DMC, de Souza LEB, et al. Engineering NK-CAR.19 cells with the IL-15/IL-15Rα complex improved proliferation and anti-tumor effect in vivo. Front Immunol 2023;14:1226518.

[26] Klingemann H. The NK-92 cell line—30 years later: its impact on natural killer cell research and treatment of cancer. Cytotherapy 2023;25:451–7.

[27] Lorenzo-Herrero S, Sordo-Bahamonde C, Gonzalez S, López-Soto A. CD107a degranulation assay to evaluate immune cell antitumor activity. Methods Mol Biol 2019;1884:119–30. | PMID: 30465198.

[28] Natividad KDT, Junankar SR, Redzwan NM, Nair R, Wirasinha RC, King C, et al. Interleukin-27 signaling promotes immunity against endogenously arising murine tumors. PLoS One 2013;8:e57469.

[29] Curran MA, Geiger TL, Montalvo W, Kim M, Reiner SL, Al-Shamkhani A, et al. Systemic 4-1BB activation induces a novel T cell phenotype driven by high expression of Eomesodermin. J Exp Med 2013;210:743–55. | PMID: 23547098; PMCID: PMC3620352.

[30] Wei J, Xia S, Sun H, Zhang S, Wang J, Zhao H, et al. Critical role of dendritic cell-derived IL-27 in antitumor immunity through regulating the recruitment and activation of NK and NKT cells. J Immunol 2013;191:500–8. | PMID: 23733881.

[31] Salcedo R, Stauffer JK, Lincoln E, Back TC, Hixon JA, Hahn C, et al. IL-27 mediates complete regression of orthotopic primary and metastatic murine neuroblastoma tumors: role for CD8+ T cells. J Immunol 2004;173:7170–82. | PMID: 15585838.

[32] Liu Z, Liu J-Q, Talebian F, Wu L-C, Li S, Bai X-F. IL-27 enhances the survival of tumor antigen-specific CD8+ T cells and programs them into IL-10-producing, memory precursor-like effector cells. Eur J Immunol 2013;43:468–79.

[33] Hemati M, Rasouli Nejad Z, Shokri M-R, Ghahremanfard F, Mir Mohammadkhani M, Kokhaei P. IL-27 impact on NK cells activity: Implication for a robust anti-tumor response in chronic lymphocytic leukemia. Int Immunopharmacol 2020;82:106350.

[34] Owaki T, Asakawa M, Fukai F, Mizuguchi J, Yoshimoto T. IL-27 induces Th1 differentiation via p38 MAPK/T-bet- and intercellular adhesion molecule-1/LFA-1/ERK1/2-dependent pathways1. J Immunol 2006;177:7579–87.

[35] Jia H, Dilger P, Bird C, Wadhwa M. IL-27 promotes proliferation of human leukemic cell lines through the MAPK/ERK signaling pathway and suppresses sensitivity to chemotherapeutic drugs. J Interferon Cytokine Res 2016;36:302–16. | PMID: 27119567; PMCID: PMC4854210.

[36] Guo Y-J, Pan W-W, Liu S-B, Shen Z-F, Xu Y, Hu L-L. ERK/MAPK signalling pathway and tumorigenesis. Exp Ther Med 2020;19:1997–2007. | PMID: 32104259; PMCID: PMC7027163.

[37] Brint E, O'Callaghan G, Houston A. Life in the Fas lane: differential outcomes of Fas signaling. Cell Mol Life Sci 2013;70:4085–99.

[38] Bui TM, Wiesolek HL, Sumagin R. ICAM-1: a master regulator of cellular responses in inflammation, injury resolution, and tumorigenesis. J Leukoc Biol 2020;108:787. | PMID: 32182390.

[39] Elkon KB, Briggs TA. The (Orf)ull truth about IRF5 and type I interferons in SLE. Nat Rev Rheumatol 2020;16:543–4. | PMID: 32709997.

[40] Barrow AD, Martin CJ, Colonna M. The natural cytotoxicity receptors in health and disease. Front Immunol 2019;10:909.

[41] Cullen SP, Brunet M, Martin SJ. Granzymes in cancer and immunity. Cell Death Differ 2010;17:616–23.

[42] de Poot S aH, Bovenschen N. Granzyme M: behind enemy lines. Cell Death Differ 2014;21:359–68.

[43] Becknell B, Caligiuri MA. Interleukin-2, interleukin-15, and their roles in human natural killer cells. Adv Immunol 2005;86:209–39 10.1016/S0065-2776(04)86006-1.

[44] Ran GH, Lin YQ, Tian L, Zhang T, Yan DM, Yu JH, et al. Natural killer cell homing and trafficking in tissues and tumors: from biology to application. Sig Transduct Target Ther 2022;7:1–21.

[45] Jamali A, Hadjati J, Madjd Z, Mirzaei HR, Thalheimer FB, Agarwal S, et al. Highly efficient generation of transgenically augmented CAR NK cells overexpressing CXCR4. Front Immunol 2020;11:2028.

[46] Levy E, Reger R, Segerberg F, Lambert M, Leijonhufvud C, Baumer Y, et al. Enhanced bone marrow homing of natural killer cells following mRNA transfection with gain-of-function variant CXCR4R334X. Front Immunol 2019;10:1262.

[47] Grzywacz B, Moench L, McKenna D, Tessier KM, Bachanova V, Cooley S, et al. Natural killer cell homing and persistence in the bone marrow after adoptive immunotherapy correlates with better leukemia control. J Immunother 2019;42:65–72. | PMID: 30489431; PMCID: PMC6365204.

[48] Li Z, Simin L, Jian K, Xin G, Youlin K. 4-1BB antibody enhances cytotoxic activity of natural killer cells against prostate cancer cells via NKG2D agonist combined with IL-27. Immunotherapy 2022;14:1043–53.

[49] Bartkowiak T, Jaiswal AR, Ager CR, Chin R, Chen C-H, Budhani P, et al. Activation of 4-1BB on liver myeloid cells triggers hepatitis via an interleukin-27 dependent pathway. Clin Cancer Res 2018;24:1138–51. | PMID: 29301830; PMCID: PMC6752715.

[50] Tam YK, Miyagawa B, Ho VC, Klingemann HG. Immunotherapy of malignant melanoma in a SCID mouse model using the highly cytotoxic natural killer cell line NK-92. J Hematother 1999;8:281–90. | PMID: 10417052.

[51] Yan Y, Steinherz P, Klingemann HG, Dennig D, Childs BH, McGuirk J, et al. Antileukemia activity of a natural killer cell line against human leukemias. Clin Cancer Res 1998;4:2859–68. | PMID: 9829753.

[52] Zhang C, Burger MC, Jennewein L, Genßler S, Schönfeld K, Zeiner P, et al. ErbB2/HER2-specific NK cells for targeted therapy of glioblastoma. J Natl Cancer Inst 2016;108(5). https://doi.org/10.1093/jnci/djv375. | PMID: 26640245.